LYMPHOID NEOPLASIA

Viral latency locus augments B-cell response in vivo to induce chronic marginal zone enlargement, plasma cell hyperplasia, and lymphoma

Sang-Hoon Sin and Dirk P. Dittmer

Department of Microbiology and Immunology and Lineberger Comprehensive Cancer Center, Center for AIDS Research, The University of North Carolina at Chapel Hill, Chapel Hill, NC

Key Points

- Kaposi sarcoma associated herpesvirus miRNAs and latent proteins drive B-cell proliferation.
- Viral miRNAs and latent proteins induce BCR and TLR hyper-responsivness in transgenic mice.

Kaposi sarcoma (KS) is associated with KS-associated herpesvirus (KSHV). This virus also causes B-cell lymphoma and B-cell hyperplasia. There exists no in vivo model for KSHV-associated B-cell malignancies or premalignant persistence in B cells. We generated a transgenic mouse that expresses multiple viral latent genes, including LANA, vFLIP, vCYC, all viral micro RNAs, and kaposin under the transcriptional control of their natural regulatory region. This promoter is B-cell specific, though it is a weak promoter. Mature B cells were chronically activated, leading to hyperglobulinemia triggered by increased plasma cell frequency and marginal zone (MZ) B-cell hyperplasia. The mice had an augmented response to T-dependent antigen as well as the TLR4 ligand LPS, leading to exacerbated MZ and germinal center responses and increased CD138$^+$ plasma cells. It is the first model to assess the viral micro RNA function in vivo. These data support a potentially novel mechanism of viral persistence in which virally infected B cells become hyper-responsive to coincident, but unrelated, pathogen exposure, leading to preferential expansion and ultimately lymphoma in a small subset of cases. (*Blood*. 2013;121(15):2952-2963)

Introduction

Kaposi sarcoma (KS)-associated herpesvirus (KSHV) is a lymphotropic γ herpesvirus. KSHV has been implicated in the pathogenesis of KS, which is the most frequent cancer in HIV-infected patients and the third most frequent cancer overall in sub-Saharan countries, where KSHV is acquired in childhood.[1] African, or endemic, KS predates the emergence of AIDS-KS, much like endemic Epstein-Barr virus (EBV)-associated Burkitt lymphoma (BL) antecedes the emergence of HIV-associated BL. KSHV is linked to B lineage lymphotropic disorders, specifically primary effusion lymphoma (PEL), the plasmablastic variant of multicentric Castleman disease, and instances of diffuse large B-cell lymphoma.[2,3] Novel epidemiologic evidence now invites the speculation that KSHV infection contributes to marginal zone (MZ) lymphoma (MZL).[4]

The main target for KSHV infection is the B cell.[5,6] Though KSHV also infects other cells, in vivo long-term latency has only been observed in B cells.[7] Thus, we investigated the B-cell developmental stage at which KSHV exerts its pathological drive. Multiple genes are expressed during KSHV latency. These include the latency-associated nuclear antigen (LANA), a cellular cyclin D2 homolog (vCYC), K13 (vFLIP), K12 (kaposin), and all viral micro RNAs (miRNAs).[8,9] Earlier, we reported transgenic mice that express a single viral protein, LANA using its own B-cell specific promoter.[10,11] In 100% of the mice, the expression of LANA augmented the B-cell response to a T-dependent (TD) antigen[12]; the mice developed splenic follicular (FO) hyperplasia, a fraction of which progressed to B-cell lymphoma.[10] Transgenic mice expressing another KSHV latent gene, K13, developed B-cell lymphoma over a 30-mo period; another strain of K13 transgenic mice failed to develop germinal centers (GCs).[13,14] Elevated expression of only vCYC in transgenic mice led to apoptosis. It led to lymphoma only in a p53$^{-/-}$ background.[15] This suggests that multiple viral genes cooperate to bring about B lineage persistence and lymphomagenesis. These proteins and viral miRNAs are expressed in KSHV-infected human B cells and PEL.[16,17] Therefore, we generated transgenic mice that express this complete complement of core KSHV latent genes, including for the first time all viral miRNAs within the mature, naïve B-cell compartment.

There are 3 subsets of B lymphocytes: B-1, FO, and MZ B cells. B-1 cells are further divided into B-1a and B-1b cells based on expression of CD5 and anatomical localization.[18] FO B cells participate in eliciting the immune response to T-cell–dependent antigens, whereas MZ and B-1 B cells respond to T-cell–independent, multivalent antigens, including LPS.[19] Circulating FO B cells home to B-cell follicles, which are juxtaposed to the T-cell zone. Activated B and T cells communicate with each other at this interface to initiate T-cell–dependent responses. FO B cells are recirculated around bone marrow (BM) sinusoids and can also display T-cell–independent immune responses.[20,21] Unlike circulating FO B cells, B-1 and MZ B cells reside in specialized locations and exhibit immunoglobulin (Ig)M responses independent of T-cell help.[22] However, MZ B cells are a heterogeneous population. They can

Submitted March 6, 2012; accepted December 26, 2012. Prepublished online as *Blood* First Edition paper, January 30, 2013; DOI 10.1182/blood-2012-03-415620.

The online version of this article contains a data supplement.

The publication costs of this article were defrayed in part by page charge payment. Therefore, and solely to indicate this fact, this article is hereby marked "advertisement" in accordance with 18 USC section 1734.

also respond to T-cell–dependent antigen.[23] Lastly, natural antibodies, which are secreted in the absence of antigen stimulation, are produced by B-1 and MZ B cells without antigen stimulation and recognize epitopes on microbial pathogens.[24,25] This propensity was augmented in the KSHV latency transgenic mice.

The KSHV latency locus drove high-level B-cell activation and MZ B-cell expansion. Transgenic B cells showed an enhanced response to TD antigen, acute activation of MZ, and augmented GC response to LPS. This supports a model of pathogen synergy where infection with the second, unrelated pathogen increases the persistence of this B-cell tropic virus.

Methods

Transgenic mice

The sequence encompassing KSHV latency locus (nt. 116 207-132 230), except vIRF-3, was cloned into the *Not*I site of pBACe3.6. The transgene fragment was injected into fertilized embryos of C57BL/6 mice and transgenic mice were generated by the Animal Models Core Facility at the University of North Carolina at Chapel Hill. All experiments were approved by the Institutional Animal Care and Use Committees at The University of North Carolina at Chapel Hill. Real-time quantitative polymerase chain reaction (qPCR) and Southern blotting were performed as previously described.[12] Gel electrophoresis for confirming real-time qPCR was carried out using the LabChip system (Caliper, Hopkinton, MA). Real-time reverse transcription (RT)-qPCR for KSHV pre-miRNAs was conducted as described[16] and confirmed by Bioanalyzer (Agilent, Santa Clara, CA). Mature KSHV miRNAs were detected using a TaqMan assay (Applied Biosystems, Foster City, CA). RNA was isolated from spleens of transgenic or wild-type mice for RT-qPCR.

Flow cytometry

Flow cytometry was performed as previously described.[12] In brief, single-cell suspensions were obtained from mouse spleens or Peyer's patches or mesenteric lymph nodes by pressing through a 40-μm cell strainer and lysing erythrocytes with buffered ammonium chloride. Cells were stained at 5×10^6 cells/mL on ice for 1 h in the dark with fluorochrome-conjugated antibodies in phosphate-buffered saline (PBS) containing 3% fetal bovine serum. Data were acquired on a CyAn instrument (Beckman Coulter, Indianapolis, IN) and analyzed using FlowJo (Tree Star, Ashland, OR).

Immunohistochemistry

Immunohistochemistry assays were done as described with modifications.[10,12,26] In brief, mouse spleen was frozen in TFM Tissue Freezing Medium (Triangle Biomedical Sciences). Then 6-μm sections were prepared using a cryotome (Leica CM1850 UV). For metallophilic macrophages (MOMA-1), peanut agglutinin (PNA), and CD45R (B220) detection, sections were fixed in cold acetone for 10 min and blocked in PBS containing 10% fetal bovine serum followed by overnight incubation with appropriate primary antibodies at 4°C. After washing with a wash buffer (PBS containing 0.05% Triton X-100), slides were incubated with secondary antibody for 2 h at room temperature. Finally, slides were washed 3 times with wash buffer and mounted using VECTASHIELD mounting medium (Vector Laboratories) as previously described.[12] Hematoxylin and eosin, kaposin, and vCYC staining were visualized using a microscope (Leica DMLS, Germany). The magnifications of the objective lenses were ×10 or ×40. Images were captured using a camera (Leica DFC480) and acquired using FireCam (Version 3.0, Leica). Immunofluorescent staining images were visualized using a fluorescent microscope (Leica DM4000B). The magnification of the objective lenses was ×20. Images were captured using a camera (QImaging RETIGA-2000RV, Surrey, BC, Canada) and analyzed using SimplePCI (Version 6.2, Compix Inc., Imaging Systems, Sewickley, PA).

Antibodies and reagents used for flow cytometry and immunohistology

The following antibodies were used: anti-vCYC, biotinylated MOMA-1 (Abcam), rat mAb to LANA (Advanced Biotechnologies Inc.), Alexa Fluor 488-conjugated anti-B220, fluorescein isothiocyanate-conjugated anti-mouse activation antigen GL7, anti-mouse IgD, phycoerythrin (PE)-conjugated anti-mouse CD21/CD35, anti-mouse IgM, PE/Cy5.5-conjugated anti-mouse CD45R, PE-conjugated anti-mouse CD138 (BD Biosciences), Alexa Fluor 555-conjugated anti-rat IgG antibodies (Cell Signaling Technology), Alexa Fluor 488-conjugated streptavidin, Alexa Fluor 555-conjugated streptavidin, allophycocyanin-conjugated anti-mouse CD19, anti-mouse CD23, fluorescein isothiocyanate-conjugated anti-mouse CD24, anti-mouse CD45R (B220), anti-mouse CD69, and PE-conjugated anti-mouse CD86 (Invitrogen), anti-kaposin (Millipore), PE-conjugated mouse anti-major histocompatibility complex class II (Miltenyi), and biotinylated PNA (Vector Laboratories).

B-cell isolation and proliferation

B cells were aseptically purified from a mouse spleen via elimination of non-B cells using an EasySep Mouse B Cell Enrichment Kit (Stemcell). The percentage of purified B cells was 96% to 97% when assessed by flow cytometry (data not shown). Purified B cells were cultured in RPMI 1640 medium supplemented with 20% fetal bovine serum, 2 mM L-glutamine, penicillin (0.05 μg/mL), and streptomycin (5 U/mL) (Invitrogen) with LPS (from *Escherichia coli* 0111:B4; Invivogen), CD40 mAb (clone HM40-3, Biolegend), or $F(ab')_2$ goat anti-mouse IgM Ab (Jackson ImmnuoResearch Laboratory) at 37°C under 5% CO_2. The ex vivo cell proliferation rate was determined by incorporation of 5-ethynyl-2′-deoxyuridine (EdU) into DNA using a Click-iT EdU microplate assay kit (Invitrogen) according to the manufacturer's guide.

In vivo LPS stimulation

KSHV latency transgenic and littermate control mice were intraperitoneally administered with either PBS or 10 μg LPS/mouse (from *Escherichia coli* 0111:B4; Invivogen). On d 1 and 7, splenic B cells were prepared and cultured with LPS. Proliferation was measured as described above.

Immunization

For analysis of primary immune response, transgenic and littermate control mice (11–13 wk old) were immunized intraperitoneally with 100 μg alum-precipitated 4-hydroxy-3-nitrophenylacetyl-keyhole limpet hemocyanin (NP_{30}-KLH) or NP_{23}-CGG (Biosearch Technologies Inc.) in 0.1 mL saline or 0.1 mL saline (mock). To assess the secondary immune response, mice (8-12 wk old) were immunized with 100 μg alum-precipitated NP_{30}-KLH on d 0 and boosted on d 21 and 42.

ELISA

To determine TD antigen-specific primary immune response, serum was prepared on d 0 (before immunization), 1, 5, and 14. Amounts of KLH-specific IgM and IgG in the serum were measured by ELISA (Life Diagnostics). For analysis of secondary TD-specific immune response, mice were bled on d 0 (before immunization), 5, 14, 26, and 49. To measure the concentration of resting or NP-specific antibodies of Ig isotypes, either unlabeled anti-mouse Ig antibodies (Southern Biotech) or NP_{34}-BSA (Biosearch Technologies) were used for coating microtiter plates. Alkaline phosphatase-conjugated antibodies and *p*-nitrophenyl phosphate were used for detection (Southern Biotech). For evaluating affinity maturation of each Ig isotype, the binding ratio to NP_9-BSA and NP_{34}-BSA was determined by titrating each serum on both the high and low haptenated proteins.

Detection of Ig gene rearrangements

Ig heavy chain gene rearrangements were detected as previously described.[10] The intensity of each PCR band was quantified using the LabChip system.

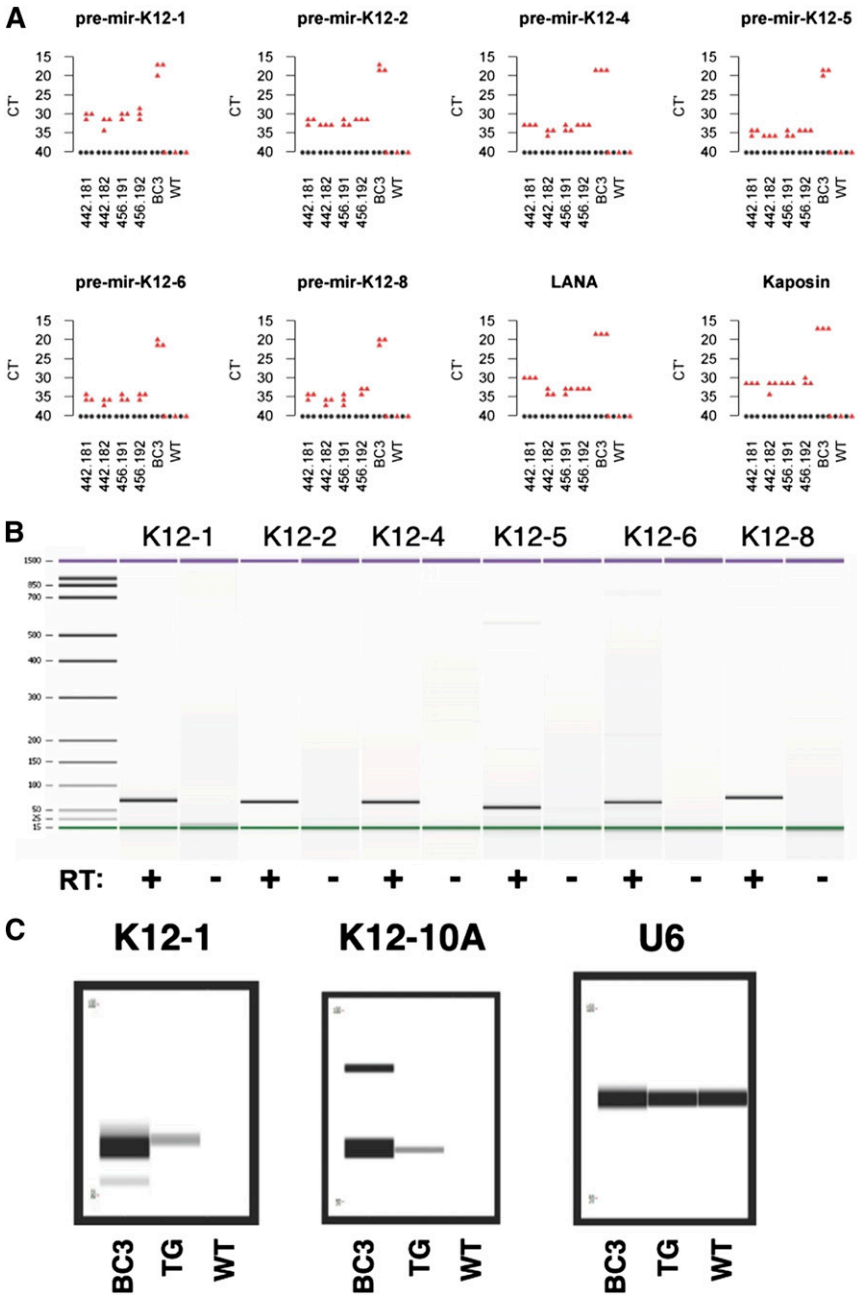

Figure 1. Transcription of KSHV miRNAs. (A) Transcription of pre-miRNAs and other transgenes was represented as RT-qPCR Ct values from 2 transgenic mice from 2 independent lines or a wild-type (WT) mouse. BC3, a PEL cell line, was used as a positive control. (B) Transcription of pre-miRNAs was validated using Bioanalyzer. RT+ and RT− represent RT-PCR reactions and reactions without reverse transcriptase, respectively. (C) Expression of mature miRNAs was confirmed using the TaqMan assay. Amplified products were visualized via the LabChip system. BC3, a PEL cell line was used as a positive control and U6 was used as a positive control for TaqMan assay system.

Statistical analysis

The mean and standard deviation are reported. Data were compared using 2-tailed Student *t* tests. Differences were considered significant if $P \leqslant .05$.

Results

Constitutive immune activation in KSHV latency locus transgenic mice

KSHV LANA alone induces FO B-cell hyperplasia in transgenic mice.[10] Because LANA is only one of multiple viral latent genes, we hypothesized that the KSHV latent genes collaborate to reprogram latently infected B cells. To test this hypothesis, we generated KSHV latency locus transgenic mice. Mice were generated by pronuclear injection of a 16 023-bp DNA fragment, which comprises LANA, vCYC, K13, all KSHV miRNAs including the viral miR-155 ortholog, and K12 (supplemental Figure 1A). Transgene integration was validated by Southern blot (supplemental Figure 1B). Multiple independent founder lines were obtained (supplemental Figure 1C). Genotyping was done by PCR. The transgene fragment was amplified from all transgene-positive mice but not littermate controls (supplemental Figure 1D). Transgene mRNA was detectable using probes for either the most 5′ gene LANA or the most distal 3′ gene kaposin (Figure 1A). Expression of KSHV pre-miRNAs was confirmed using qRT-PCR (Figure 1A). The qRT-PCR products exhibited the predicted size and were dependent on RT (Figure 1B).

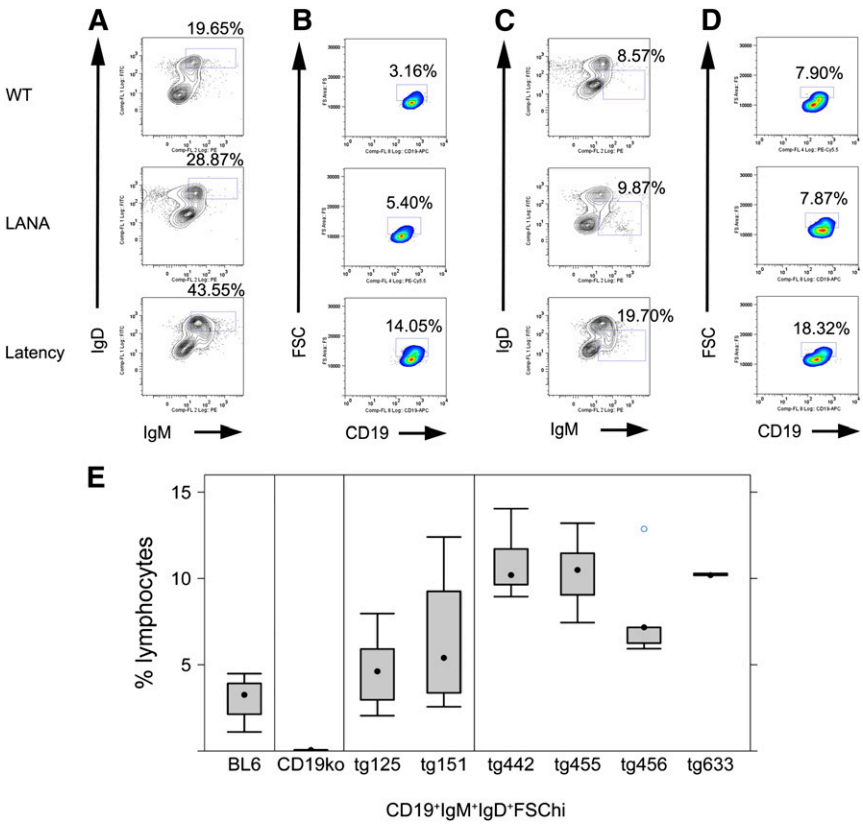

Figure 2. Phenotype of KSHV latency locus transgenic mice. Splenocytes were subject to flow cytometric analyses. (A) Representative mature B-cell profiles from wild-type (WT), KSHV LANA transgenic (LANA), and KSHV latency locus transgenic mouse (Latency). Percentages of IgD^+IgM^+ lymphocytes among whole lymphocytes are indicated above each gate. (B) Profiles of activated (FSChi) mature B cells are shown. Gates represent $CD19^+IgD^+IgM^+$FSChi-activated B cells. (C) MZ B cells are gated as IgD^-IgM^+. (D) Activated MZ B cell ($CD19^+IgD^-IgM^+$FSChi) profiles are shown. (E) Comparison of activated mature B cells defined as $CD19^+IgD^+IgM^+$FSChi from WT (n = 9), ko (CD19 knockout, n = 4), LANA (KSHV LANA transgenic, n = 13), and latency (KSHV latency locus transgenic, n = 23) mice. tg125 (n = 8) and tg151 (n = 5) mean 2 independent lines of the KSHV LANA transgenic mice. tg442 (n = 9), tg455 (n = 6), tg456 (n = 5), and tg633 (n = 3) represent 4 independent lines of the KSHV latency locus transgenic mice.

Processing to and expression of mature miRNAs in the transgenic mice was confirmed by TaqMan assay (Figure 1C). Expression of the kaposin protein was confirmed on Peyer's patches from the KSHV latency transgenic mice by immunohistochemical staining (supplemental Figure 2). Expression of vCYC protein was confirmed in spleen sections from transgenic mice but not littermate controls (supplemental Figure 3). Although we were able to detect these proteins by in situ methods, their level was below the limit of detection by western blot of whole spleen lysates. The expression level of vCYC and K12 was weaker than other models, which used strong artificial promoters rather than the native viral promoter.[27,28] We did not have an antibody to detect vFLIP. LANA protein could not be detected using either immunoprecipitation-western blot or immunohistochemical assays. At present, we do not know the reason. One could speculate that the structural uniqueness of LANA, such as the large repetitive regions, affects its expression (reviewed in Ballestas and Kaye[29]). Alternatively, we noted that the LANA translation start site/KOZAK sequence is suboptimal and may be only minimally active in primary mouse B cells compared with PEL.

To characterize the effect of the KSHV latency locus on B-cell development, we analyzed frequencies and absolute cell numbers of splenic or BM B-cell populations from transgenic mice and littermate controls by flow cytometry (Figure 2; Table 1). We followed previous reports for gating schemes and markers to define each B-cell subset.[10,12,30] Mature and activated mature B cells were increased. This phenotype was much more robust compared with LANA single transgenic mice. KSHV latency locus transgenic mice harbored up to 43% mature B cells ($CD19^+IgD^+IgM^+$) (Figure 2A), whereas LANA transgenic mice averaged 25% and wild-type C57BL/6 mice had only 22%. Activated mature B cells ($CD19^+IgD^+IgM^+$FSChi) were increased to >10% in 4 independent lines of latency transgenic mice compared with <5% in littermate controls (Figure 2B,E). An analysis on absolute numbers of gated cells was consistent with that on cell frequencies (Table 1; supplemental Fig 4). Levels of MHC class II and CD69 were also analyzed by flow cytometry, but there was no significant difference between the transgenic and littermate control mice (data not shown). To examine if B cells from the KSHV latency transgenic mouse show hyper-responsiveness to lower doses of B-cell stimulators, splenic B cells from the transgenic or littermate control mice were cultured with anti-IgM or anti-CD40 antibodies, or LPS and proliferation was quantified by EdU uptake. Transgenic B cells proliferated more than wild-type B cells following CD40 or T-independent antigen stimulation, indicating sensitization of the CD40 pathway and T cell-independent B-cell activation pathway in the KSHV latency locus transgenic mice (supplemental Figure 5). This demonstrated constitutive immune activation and hyperplasia in the presence of the normal environmental flora alone.

MZ expansion and increased frequency of plasma cells in KSHV latency locus transgenic mice

The second, qualitative novel phenotype was an increase in MZ B cells. MZ B cells ($CD19^+IgM^+IgD^-$) were significantly increased in the spleens of all latency locus transgenic mice (Table 1; Figure 2C). Activated MZ B cells were similarly increased (Figure 2D). This was confirmed by histology, which evidenced significantly enlarged MZs in transgenic compared with littermate control mice (supplemental Figure 6). This MZ expansion was not found in LANA single transgenic mice. This suggests that multiple KSHV latent genes cooperate to lower the initial activation threshold of a specific subset of B lineage cells, which are involved in initial pathogen recognition.

To further confirm the MZ expansion in the latency locus transgenic mice, we performed 4-color flow cytometry. Splenic

Table 1. B-cell populations in KSHV latency locus transgenic mice

		Frequency							Absolute numbers				
		Wild-type			KSHV latency tg				Wild-type		KSHV latency tg		
Class	Marker	%	SD	n	%	SD	n	P	#	SD	#	SD	P
Mature	CD19+IgM+IgD+	22.08	7.34	9	36.00	6.36	9	0.01	3717	1182	6197	1710	0.003
Activated B	CD19+IgM+IgD+FSC-hi	4.82	2.14	9	9.54	2.44	9	0.0003	783	326	1859	555	0.0002
MZ	CD19+IgM+IgD-	11.83	3.12	9	15.75	2.21	9	0.01	1974	390	3028	376	0.00003
Activated MZ	CD19+IgM+IgD-FSC-hi	2.57	1.14	9	4.47	1.48	9	0.009	429	160	857	276	0.001
MZ	CD19+CD21hiCD23-CD24+	2.25	0.23	6	3.69	1.01	9	0.002	352	36	592	168	0.002
MZ	CD19+CD21hiCD23-IgD-	1.07	0.32	6	1.75	0.63	9	0.02	182	53	281	111	0.04
GC	CD19+IgD-CD21-CD23+	0.46	0.27	6	0.35	0.13	9	NS	72	42	56	20	NS
NF/T1	CD19+CD21intCD23-IgDlo	1.52	0.45	6	1.31	0.38	9	NS	241	71	210	59	NS
T2-FP	CD19+IgD+CD21intCD23+	31.24	5.75	6	28.84	6.62	9	NS	4980	944	4627	1048	NS
T2-MZP	CD19+IgD+CD23+CD21hi	4.12	0.90	6	5.41	1.09	9	0.03	655	135	867	170	0.02
FO	CD19+IgD+IgMloCD23+	4.24	0.97	7	4.05	1.50	11	NS	672	147	696	235	NS
B-1a	CD19+B220+CD5+	0.52	0.29	9	0.76	0.27	9	NS	111	50	116	53	NS
Plasma (spleen)	CD19-B220-CD138+	0.89	0.19	5	1.32	0.28	5	0.02	504	86	1106	152	0.0002
Plasma (BM)	CD19-B220-CD138+	0.17	0.07	6	0.47	0.18	6	0.004	37	12	115	44	0.006

#Absolute number of the gated cells.

hi, high; int, intermediate; lo, low; NF/T1, newly formed or transitional type 1; NS, not significant; T2-FP, transitional type 2-follicular precursor B cell; SD, standard deviation; tg, transgenic.

cells were first gated using CD19 and CD24. Double positive cells were further gated with CD21 and CD23. MZ B cells ($CD19^+CD24^+CD21hiCD23^-$) were significantly increased in the transgenic mice compared with wild-type mice (Figure 3A,C; $P \leq .002$, Student t test; n = 9). This result was corroborated using a second marker set; $CD19^+IgD^-CD21hiCD23^-$ cells were increased in KSHV latency locus transgenic mice compared with nontransgenic littermates (Figure 3B,C; $P \leq .02$, Student t test; n = 9).

The in situ expansion of MZ B cells was analyzed by immunofluorescence assay. Spleen sections from the transgenic mice and age-matched littermate controls were stained using MOMA-1 and the pan B cell marker B220. MOMA-1 marks the interface between the B-cell follicle and the MZ. The MZs were expanded in the spleens of the transgenic mice compared with those of wild-type mice. Specifically, MZ B cells stained with B220 were more enlarged outside the MOMA-1 ring (Figure 3E).

It is thought that newly formed/transitional type 1 B cells differentiate into transitional type 2-follicular precursors (T2-FPs), which develop into either MZ via transitional type 2-MZ precursors or FO B cells.[30] To evaluate how the KSHV latency locus affects precursors of MZ cells, we analyzed these populations. The newly formed/transitional type 1, T2-FP, precursors of FO B cells were not affected (Table 1). By contrast, transitional type 2-MZ precursors, which are MZ precursors and differentiated from T2-FP, were significantly increased (Figure 3D). This is the first report that implicates MZ in KSHV persistence and pathogenesis.

The third qualitative novel effect of the KSHV latency locus on mouse B-cell development is increased frequency of $CD138^+$ plasma cells in spleen ($P \leq .02$, Student t test; n = 5). This phenotype was more robust in BM ($P \leq .004$, Student t test; n = 6), showing plasmablasts ($CD19^-B220^+CD138^+$) were also increased, see Figure 5 panels C and D. This indicates KSHV latency locus augments plasma cell development in BM and spleen. This is the same lineage of B cells that in a subset of KSHV-infected patients gave rise to $CD138^+$ PEL.

KSHV latency locus augments TLR4:LPS signaling

As the latency locus-expressing mice displayed an increased number of activated mature B cells, we investigated GC formation. To identify activated GC, PNA, a well-validated activation marker for GC B cells, was used. Enlarged PNA-positive patches were found in the latency transgenic mice (Figure 4A,B). The in situ difference between wild-type and transgenic mice confirmed the quantitative subset analyses (Table 1). This striking phenotype in the absence of overt antigen exposure prompted us to directly examine the effect of the viral genes on B-cell activation. Firstly, we injected LPS to polyclonally activate B cells in vivo. Twenty-four hours later, splenocytes were analyzed by flow cytometry. Even before LPS administration, the fraction of activated GC B cells ($CD19^+CD71^+PNAhi$) was already elevated in the transgenic mice compared with the wild-type mice, consistent with our in situ observation (Figure 4C,D). LPS increased the percentage of the activated B cells in the wild-type mice, as expected, and to even higher levels in the transgenic mice (Figure 4C). LPS-dependent activation subsided by d 7 after injection in both (data not shown). Activated MZ B cells ($CD19^+CD21hiCD23^-CD69^+$) were augmented in both wild-type and the latency transgenic mice upon LPS injection (Figure 4D). However, MZ B cells were significantly more expanded by LPS in the transgenic mice compared with littermate controls ($P \leq .05$, Student t test; n = 5). The same cells were more activated as judged by mean expression of CD69 (Figure 4E). This demonstrates that KSHV latent genes augment the initial B-cell response to a polyvalent, TLR4-engaging antigen.

GC response to TD antigen

To determine the primary GC B-cell response to a strictly TD antigen, we administered NP-KLH or saline control via an intraperitoneal injection without adjuvant. Splenic cells were harvested 10 d later and analyzed using CD71 as a marker for activation. As expected, GC B cells of the transgenic mice were more activated than the wild-type mice in the absence of treatment (Figure 5A; $P \leq .04$, Student t test; n = 6). Activated GC B cells of both the wild-type and transgenic mice were increased after NP-KLH immunization (Figure 5A; $P \leq .04$, Student t test; n = 6). However, the GC B cells of the transgenic mice responded much better to NP-KLH than those of the wild-type mice (Figure 5A; $P \leq .001$, Student t test; n = 6). We independently confirmed the augmented GC response in KSHV transgenic mice by immunizing with a second

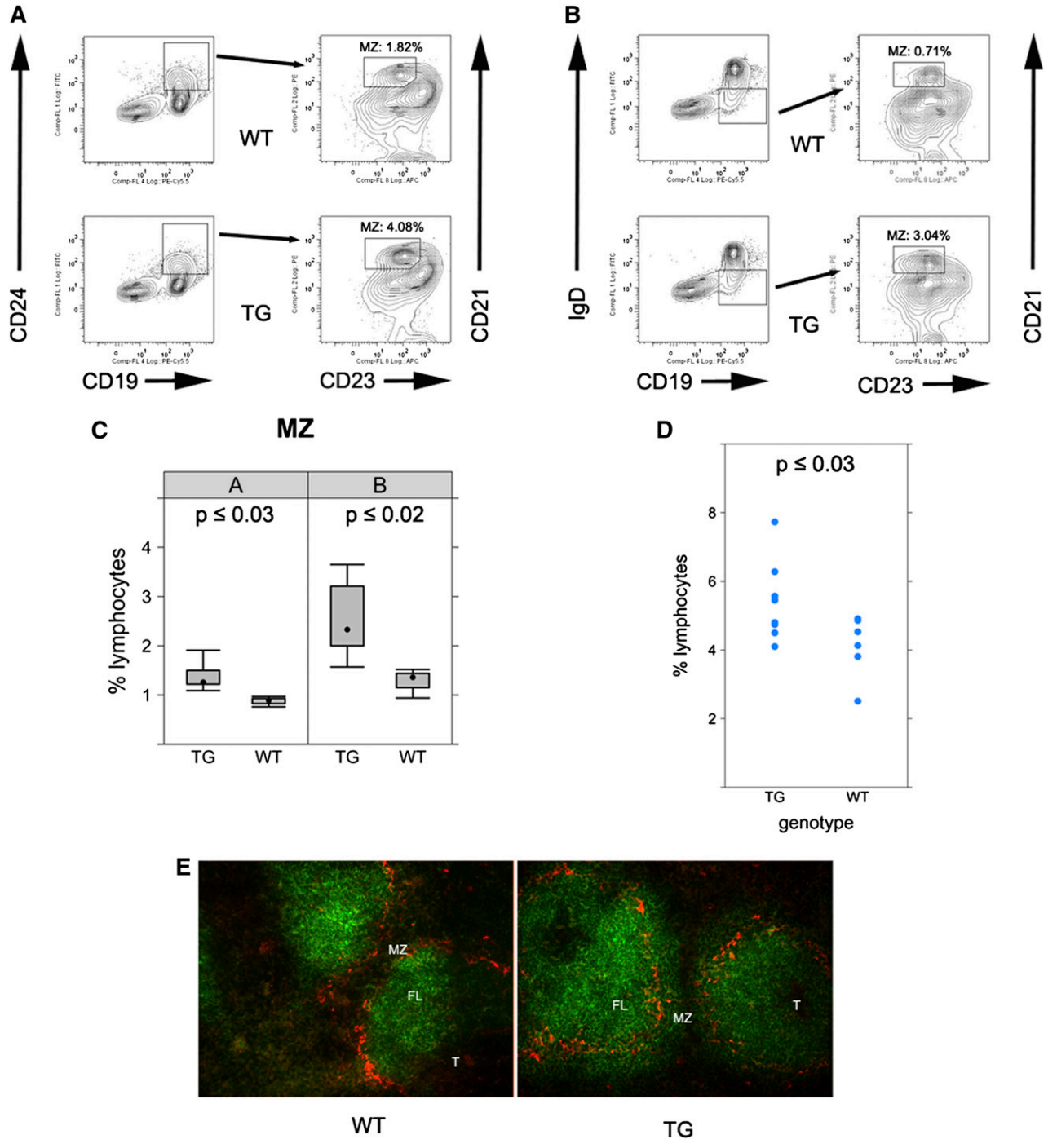

Figure 3. MZ expansion in KSHV latency locus transgenic mice. (A) Splenocytes from wild-type (WT) or latency transgenic mouse (TG) were analyzed by fluorescence-activated cell sorter (FACS). $CD19^+CD24^+$ cells were further gated with CD21 and CD23. Percentages of $CD19^+CD24^+CD21hiCD23^-$ cells among whole lymphocytes are indicated in FACS profiles. (B) Alternatively, $CD19^+IgD^-$ cells were gated with CD21 and CD23 in an independent analysis. (C) Bar plot of flow cytometry data from panels A-B (n = 5 for WT and n = 9 for the transgenic mice). (D) MZ precursor cells were gated as $CD19^+IgD^+CD21hiCD23^+$. Average percentages of 6 WT and 9 latency transgenic (TG) mice are shown with the standard deviation. (E) Frozen spleen sections were stained with B220 (green) for B cells and MOMA-1 for marginal zone macrophages (red). Magnification ×200. FL, follicle.

TD antigen, NP-chicken γ globulin ($P \leq .03$, Student t test; n = 6; supplemental Figure 7). Thus, the presence of KSHV latent genes augments the primary B-cell response to TD antigen.

A key biomarker of chronic B-cell activation and/or hyper-responsiveness is hyperglobulinemia. We measured Ig isotype levels in peripheral blood by ELISA (Figure 5B). The levels of IgG1 and IgG3 were significantly elevated in the transgenic compared with wild-type animals, whereas the levels of other isotypes were not. This is consistent with increased plasma cell frequency of the latency transgenic mice (Table 1; Figure 5C-D), verifying nonspecific expansion of the plasma cell and MZ cell compartment by the viral latency genes.

To measure the antibody response to the TD antigen, NP-KLH, we used NP- or KLH-specific ELISA. The KLH-specific IgM levels of the transgenic and wild-type mice were increased at 5 d after immunization, but there was no difference compared with

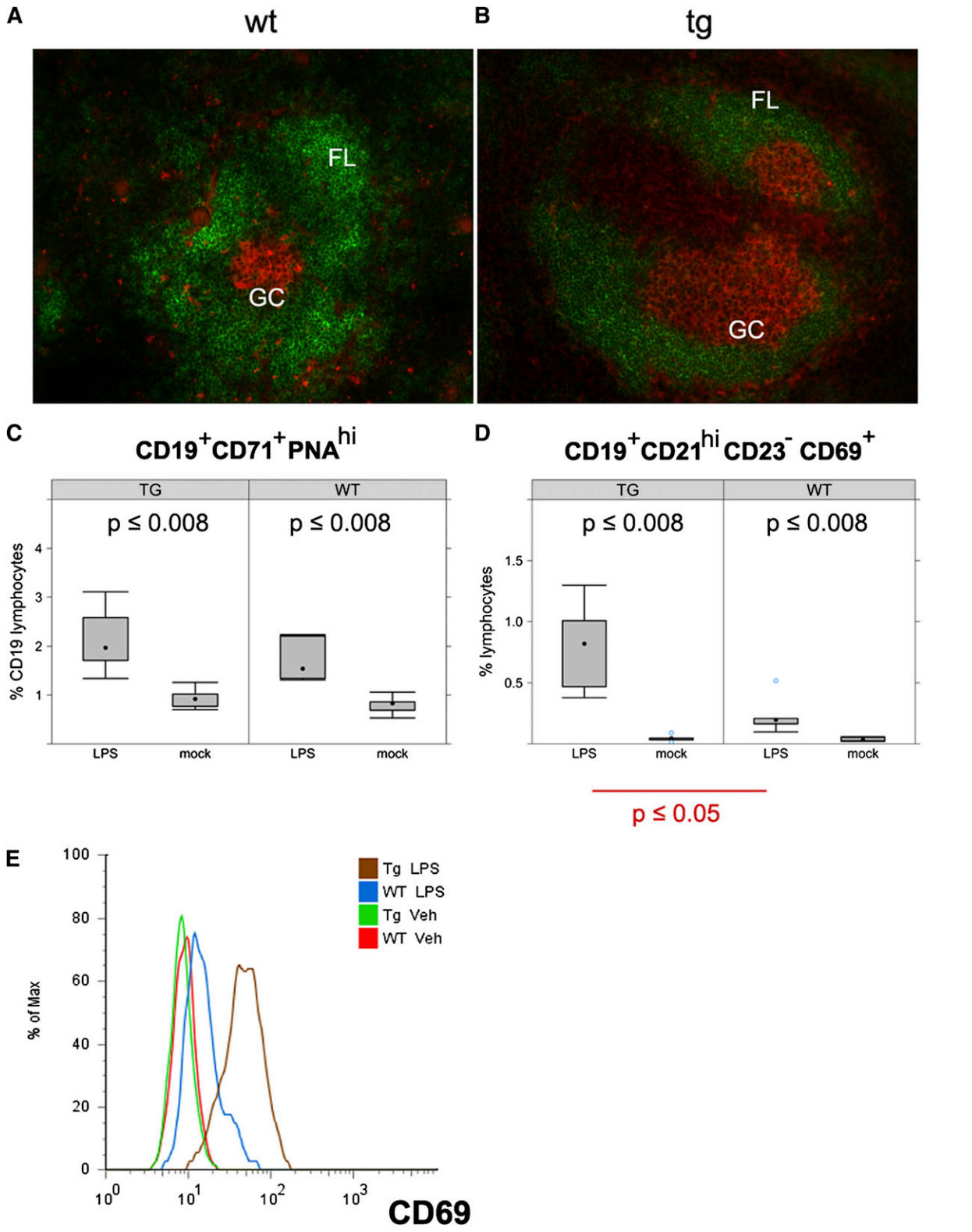

Figure 4. LPS-induced B-cell expansion in KSHV latency locus transgenic mice. (A-B) Frozen spleen sections were stained with B220 (green) and PNA (orange). Magnification ×200. KSHV latency transgenic mice were injected with LPS. On d 1 and 7 after injection, splenic cells were analyzed by fluorescence-activated cell sorter. (C-D) Percentages of activated GC B cells ($CD19^+CD71^+PNA^{hi}$) and activated MZ B cells ($CD19^+CD21^{hi}CD23^-CD69^+$) are shown on d 1 after LPS injection. Averages of 6 wild-type (WT) and 6 latency transgenic (TG/Tg) mice are indicated with the standard deviation. (E) Expression of CD69, an activation marker on the $CD19^+$CD21hi$CD23^-$ gated MZ B cells. Veh, vehicle.

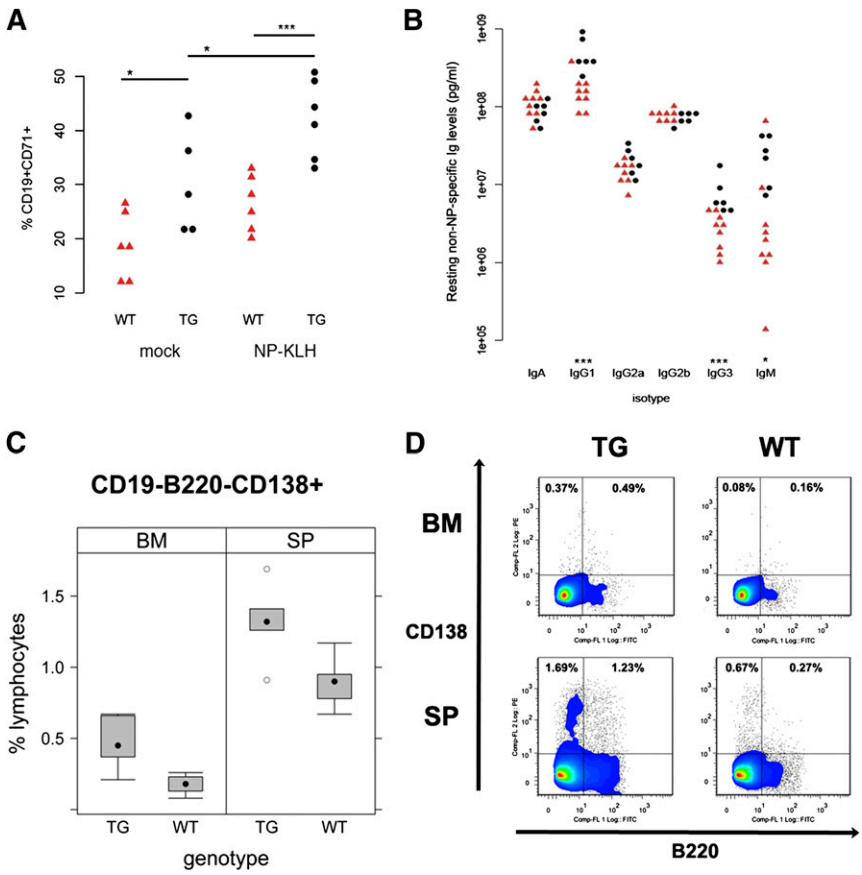

Figure 5. TD antigen-driven GC response in KSHV latency locus transgenic mice. KSHV latency locus transgenic mice and littermate controls were immunized with NP-KLH or PBS (n = 6). After 10 d, splenocytes were subject to fluorescence-activated cell sorter (FACS) analysis. Blood was collected on d 0, 5, 10, and 14. (A) Activated GC ($CD19^+CD71^+PNAhi$) are plotted. (B) Levels of resting non-NP–specific Igs of 9 wild-type (WT; red triangle) and 6 transgenic mice (black circle) were plotted on the first or second column, respectively. * and *** represent significant difference with $P < .05$ and $P < .005$ by Student *t* test, respectively. (C) The frequency of plasma cells was analyzed by FACS. Cells from spleens (SP; n = 5) or BM (n = 6) in WT or latency transgenic mice (TG) were subject to FACS. $CD19^-$ cells were further gated with B220 and CD138. Percentages of $CD19^-B220^-CD138^+$ cells among $CD19^-$ lymphocytes are plotted. (D) Representative flow cytometry profiles of plasmablasts ($CD19^-B220^+CD138^+$) and plasma cells ($CD19^-B220^-CD138^+$) from FACS analysis in (C) were shown.

the wild type (data not shown). KLH-specific IgG levels at d 5, 10, and 14 likewise were also not significantly different between wild-type and transgenic mice (data not shown). This is expected, because antigen-specific responses require T-cell help, and the frequency of helper T cells was unchanged in the transgenic mice (data not shown). To examine the effect of KSHV latency locus on the secondary immune response, class switch recombination (CSR) and somatic hypermutation (SHM), the avidity of NP-specific Ig antibodies, were determined but did not show a significant difference (data not shown). This indicates that the KSHV latency locus cannot increase CSR, SHM, or secondary immune response, all of which are limited by the amount of T-cell help. This was expected, as the transgene was not expressed in T cells (data not shown) and KSHV is not found in T cells in human patients. In sum, the KSHV latency locus induces hyperglobulinemia and augments B-cell activation in response to TD antigen, but because complete responses depend on specifically activated T cells, which are unchanged in our model and in KSHV-infected patients, CSR, SHM, or TD secondary responses were not changed.

The experimental activation of MZ and GC B cells by polyvalent (LPS) and single hapten (NP) TD antigen mimics the preneoplastic state of latent KSHV infection, because increases in mature and MZ B cells were documented in peripheral blood samples from KSHV-infected human patients with classic, HIV-negative KS,[31] and because KSHV infection was recently associated with MZL.[4] We observed the same in our mice: over time, through continued exposure to environmental antigens and, we surmise, by accumulating additional mutations, individual B-cell clones in our mice became fully tumorigenic.

Monoclonal tumor found in KSHV latency locus transgenic mice

As B cells in KSHV latency transgenic mice were consistently activated, we observed the mice for the presence of splenomegaly and lymphoma. A cohort of 79 KSHV latency transgenic and 61 littermate control mice was followed for 400 d. We evaluated lymphoid hyperplasia based on gross pathological manifestation and histological characteristics. The incidence of lymphomas in the littermate controls was 2.7% (1/37), whereas 16% (8/50) of the KSHV latency transgenic mice developed tumors (Figure 6G). This incidence was significantly higher than that of C57BL/6 mice,[10,32] because compared with other mouse strains, C57BL/6 are tumor resistant except for late onset of T-cell thymoma. We did not observe thymoma during follow-up. Spleens of tumor-bearing mice were enlarged compared with age-matched control (Figure 6A). The length of this example was 3.1 cm. The spleen architecture of the mice was histologically characterized as mainly medium to large lymphocytes with frequent mitoses and a small number of mature lymphocytes. An increased number of megakaryocytes with foci of erythroid and myeloid cells, indicating extramedullary hematopoiesis, was also observed (Figure 6E, TG), whereas spleen from a wild-type mouse consisted of mainly small lymphocytes and a small number of reticuloendothelial cells, consistent with a normal splenic architecture (Figure 6E, WT). Because the splenomegaly developed slowly and late in life, overall survival was not significantly different; however, as shown in Figure 6G, only transgenic animals developed severe (defined as greater than median + median absolute deviation) splenomegaly. This difference was statistically significant ($P \leqslant .05$).

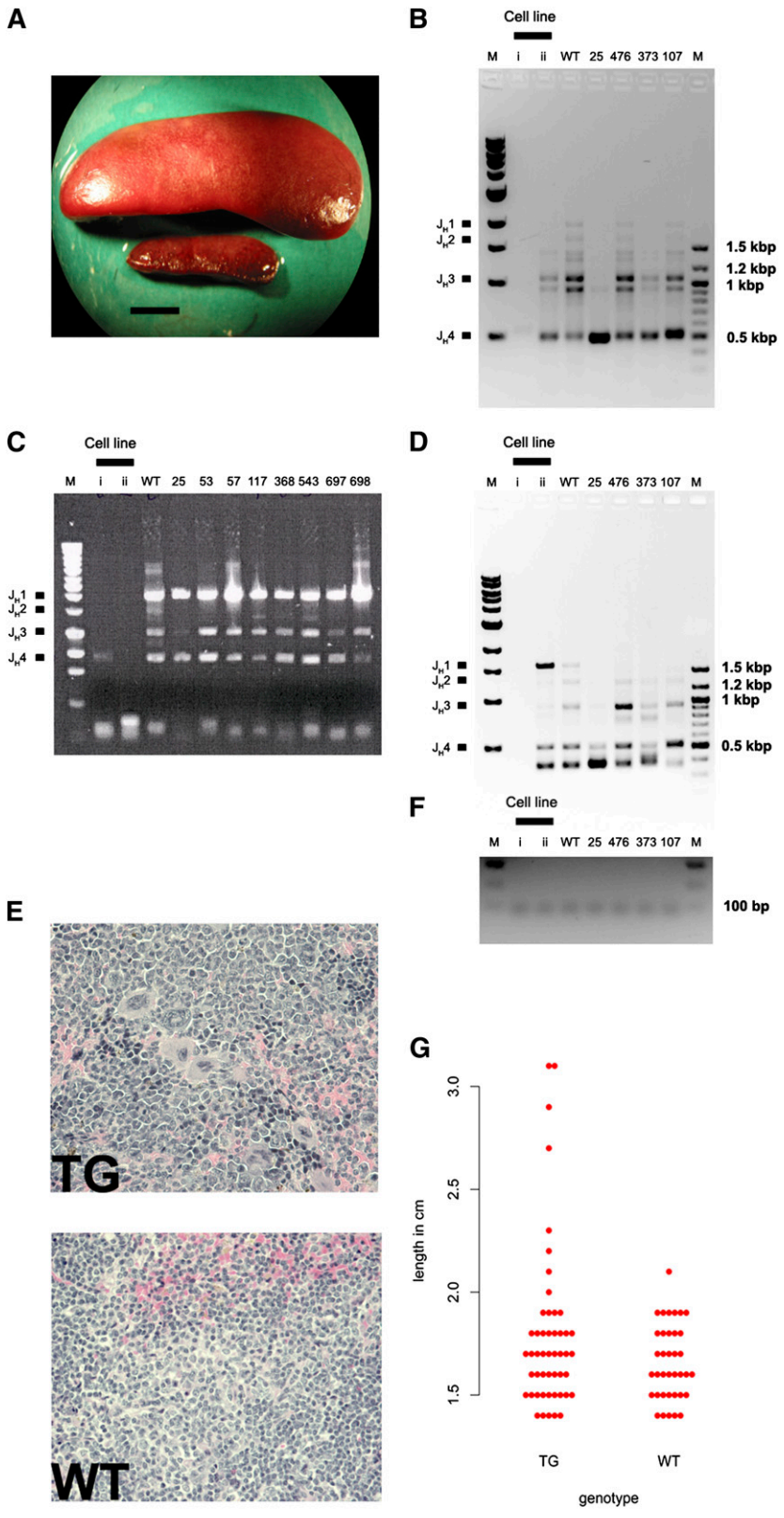

Figure 6. Monoclonal IgH rearrangement in tumors from KSHV latency locus transgenic mice was evaluated using PCR. (A) Splenomegaly found in a KSHV latency locus transgenic mouse with the spleen of a wild-type (WT) mouse. Bar represents 0.5 cm. (B-D) PCR products of splenic genomic DNAs from latency transgenic mice, 2 mouse lymphoma cell lines (i and ii), and 1 C57BL/6 mouse (WT) were resolved on a 1% Tris-acetate-EDTA-agarose gel. The WT lane shows 4 rearrangements of VDJ_H1, VDJ_H2, VDJ_H3, and VDJ_H4 (B-D) using D_H5 (B), Dq52 (C), or V_H7183 primers (D). ApoB was amplified to demonstrate an equal amount of genomic DNA was used for PCR (F). Cell lines i and ii mean mouse lymphoma cell lines; K46 and M12. M; 1-kb or 100-bp DNA ladder. Spleen architectures of the same mouse as in Figure 6A (E, TG) and littermate control mouse (E, WT) revealed by hematoxylin and eosin staining. Magnification ×400. (G) Spleen sizes of the KSHV latency transgenic (TG) and littermate control mice (WT) were plotted.

To assess clonality, Ig heavy chain gene rearrangement was analyzed by PCR. In wild-type mice, 4 bands (J_H1-J_H4) were produced with primers D_H5:J_H, V_H7183:J_H, or Dq52:J_H family rearrangements, indicative of a polyclonal mature B-cell population. By contrast, only one band was found in the mouse tumor 25 with primers D_H5:J_H or V_H7183:J_H and 2 bands with Dq52:J_H primers. The intensity of each band, which was quantified using the LabChip system, supported the PCR analysis (supplemental Figure 8). We concluded that the B-cell expansion was monoclonal (Figure 6B-D, F). Thus, one long-term consequence of consistent KSHV-induced B-cell activation is lymphomagenesis.

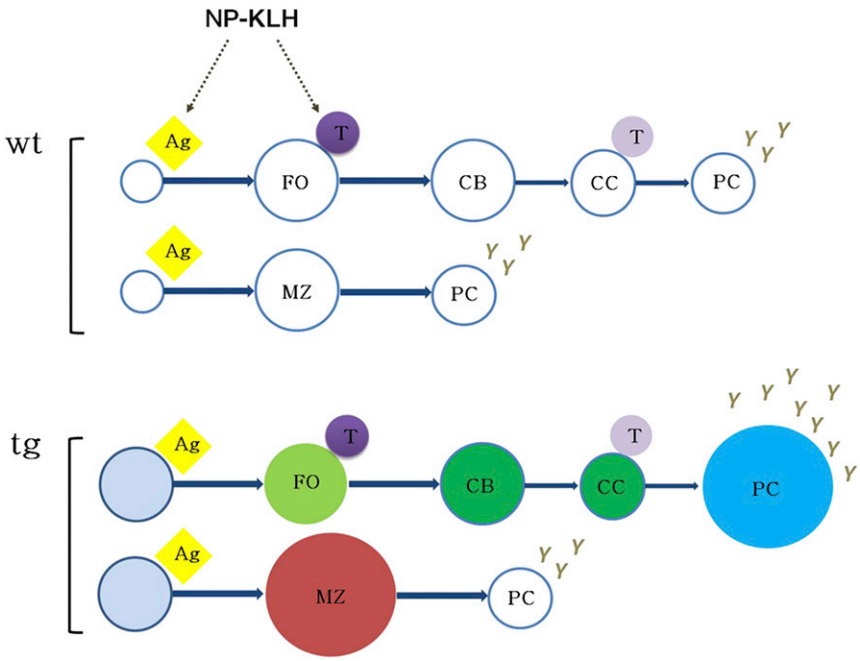

Figure 7. Model for KSHV latency locus-mediated augmentation of B-cell response. The expression of KSHV latent genes in mouse B cells results in mature B-cell activation, expansion of MZ and plasma cells, and augmented B-cell response to antigen. The status of constant B-cell activation and subsequent hyper-responsiveness to antigen in vivo suggests that KSHV latency locus serves as a chronic antigenic stimulator to the viral lymphomagenesis. Ag, antigen; CB, centroblast; CC, centrocyte; FO, follicular B cell; PC, plasma cell; T, T cell.

Discussion

Our understanding of the pathobiology of KSHV-associated lymphoproliferative diseases (PEL, multicentric Castleman disease, diffuse large B-cell lymphoma, and MZL) is limited by the paucity of adequate animal models. PEL tumor cell lines have driven our understanding of KSHV function within the heavily mutated[33] cancer cell. By contrast, we know very little as to how KSHV modulates the latently infected, normal B cells and how this virus contributes to the transition from invisible latent infection to preneoplastic hyperplasia and eventually B-cell lymphoma (reviewed in Speck and Ganem[34]). Because this herpesvirus establishes lifelong persistence in B cells, the clinically dormant phase comprises >90% of the viral life span; only in the last 10% of its existence do herpesviruses cause clinical disease. KSHV LANA single transgenic mice exhibited FO B-cell hyperplasia and augmented the B-cell response to antigen in vivo,[10,12] but frank lymphoma was rare. We therefore introduced the complete multigene latency locus into mice. It contained all but one (vIRF-3) of the viral genes that are consistently found in every KSHV latently infected B cell and in every PEL tumor cell.[9,16,17] These novel transgenic mice recapitulate the precancerous latent state of KSHV infection: 1) The KSHV latency locus consistently activated mature B cells leading to hyperglobulinemia; 2) MZ B cells in particular were activated and increased in the transgenic mice, as were $CD138^+$ plasma cells; and 3) activation of MZ and GC B cells was augmented in response to polyvalent, TLR-activating (LPS), and single hapten (NP) TD antigen. These phenotypes of the latency locus were also observed in a second, different strain background (BALB/c; data not shown).

Taken together, our data indicate that the KSHV latency locus drives not only the T-independent arm of B-cell activation by expanding MZ B cells but also the TD pathway by augmenting the NP-driven GC response plasma cell frequency, leading to sustained hyperglobulinemia. This provides a novel, genetically tractable, in vivo model for the preneoplastic state of latent KSHV infection. Even though it is too early to directly tie the MZ phenotype in our model to human KSHV infection, increases in mature and MZ B cells were recently documented in human patients with classic KS,[31] and KSHV infection has been associated with MZL in a large cohort study.[4] Of note, whereas endemic KS is a disease of HIV-negative children, no childhood lymphoma has been associated with KSHV. We observed the same kinetic for frank lymphoma in our model. Only over time, through continued exposure to environmental pathogens and, we surmise, by accumulating additional mutations, do individual B-cell clones become fully transformed (Figure 7).

MZ widening, the main phenotype of our latency locus transgenic mice, is a defining feature of MZLs in mice.[35] Evidence is growing that chronic antigenic stimulation by microbial infection such as *Helicobacter pylori*, *Campylobacter jejuni*, *Borrelia burgdorferi*, and hepatitis C virus and/or autoantigen is central to the genesis of MZL.[36-40] Continuous activation and proliferation of lymphocytes, as observed during chronic microbial infection, is a risk factor for all lymphomas,[41] including *H. pylori*-associated gastric mucosa-associated lymphoid tissue and MZL.[36,42] EBV-associated lymphomas also rely on an exogenous chronic stimulation component in which microbial pathogens do not directly transform lymphoid cells but induce continual activation of lymphocytes via chronic antigenic stimulation, for example, in response to *Plasmodium falciparum* infection.[43] We do not know if the MZ phenotype is a cell autonomous property of our transgene. We speculate that in KSHV latently infected MZ cells, exposure to the second pathogen is greatly augmented, leading to unwanted expansion and eventually MZL.

Our data are consistent with recent work by Hassman et al,[44] who reported that upon KSHV infection of purified human tonsillar B cells, a subset of cells established latency, proliferated, and displayed signs of plasmablastic differentiation in this short-term assay. Memory B cells are known as a site for lifelong latency for EBV and murine gammaherpesvirus 68 (MHV68),[45,46] though MHV68 also establishes latency in transitional B cells.[47] A role for memory B cells in maintaining KSHV has not been established and we did not observe changes in memory B cells or recall responses in our model. Rather, the increased number of tissue-resident MZ B cells in our KSHV latency transgenic mice suggests that the

spleen or another secondary lymphoid organ could be the site for KSHV latency. A tissue-resident latency reservoir would be consistent with the low frequency of circulating KSHV-positive cells in asymptomatic individuals.[48]

In conclusion, this data establishes a robust model for KSHV latent gene B cell hyperplasia and a system to study the contribution of host factors in KSHV lymphomagenesis in vivo through mouse genetics. Further, it establishes a novel function for KSHV in MZ B cell expansion, which may explain long-term, tissue-resident, latent persistence of KSHV and how it could be augmented through bacterial co-infections.

Acknowledgments

The authors thank Blossom Damania and Sang-Ryul Lee for critical reading and fruitful discussion and Yongbaek Kim for lymphoma evaluation.

This work was funded by the National Institutes of Health, National Cancer Institute (grants CA109232 and CA019014). The UNC Flow Cytometry Core Facility is supported in part by an NCI Center Core Support Grant (P30CA06086) to the UNC Lineberger Comprehensive Cancer Center.

Authorship

Contribution: S.-H.S. designed research, performed research, analyzed data, and wrote the paper; and D.P.D. designed research, analyzed data, and wrote the paper.

Conflict-of-interest disclosure: The authors declare no competing financial interests.

Correspondence: Dirk P. Dittmer, Department of Microbiology and Immunology, 804 Mary Ellen Jones, CB#7290, The University of North Carolina, Chapel Hill, NC 27599-7290; e-mail: ddittmer@med.unc.edu.

References

1. Ganem D. KSHV and the pathogenesis of Kaposi sarcoma: listening to human biology and medicine. *J Clin Invest.* 2010;120(4):939-949.
2. Cesarman E, Chang Y, Moore PS, et al. Kaposi's sarcoma-associated herpesvirus-like DNA sequences in AIDS-related body-cavity-based lymphomas. *N Engl J Med.* 1995;332(18): 1186-1191.
3. Soulier J, Grollet L, Oksenhendler E, et al. Kaposi's sarcoma-associated herpesvirus-like DNA sequences in multicentric Castleman's disease. *Blood.* 1995;86(4):1276-1280.
4. Benavente Y, Mbisa G, Labo N, et al. Antibodies against lytic and latent Kaposi's sarcoma-associated herpes virus antigens and lymphoma in the European EpiLymph case-control study. *Br J Cancer.* 2011;105(11):1768-1771.
5. Ambroziak JA, Blackbourn DJ, Herndier BG, et al. Herpes-like sequences in HIV-infected and uninfected Kaposi's sarcoma patients. *Science.* 1995;268(5210):582-583.
6. Dittmer D, Stoddart C, Renne R, et al. Experimental transmission of Kaposi's sarcoma-associated herpesvirus (KSHV/HHV-8) to SCID-hu Thy/Liv mice. *J Exp Med.* 1999;190(12): 1857-1868.
7. Dupin N, Fisher C, Kellam P, et al. Distribution of human herpesvirus-8 latently infected cells in Kaposi's sarcoma, multicentric Castleman's disease, and primary effusion lymphoma. *Proc Natl Acad Sci USA.* 1999;96(8):4546-4551.
8. Cai X, Lu S, Zhang Z, et al. Kaposi's sarcoma-associated herpesvirus expresses an array of viral microRNAs in latently infected cells. *Proc Natl Acad Sci USA.* 2005;102(15):5570-5575.
9. Dittmer D, Lagunoff M, Renne R, et al. A cluster of latently expressed genes in Kaposi's sarcoma-associated herpesvirus. *J Virol.* 1998;72(10): 8309-8315.
10. Fakhari FD, Jeong JH, Kanan Y, et al. The latency-associated nuclear antigen of Kaposi sarcoma-associated herpesvirus induces B cell hyperplasia and lymphoma. *J Clin Invest.* 2006; 116(3):735-742.
11. Jeong JH, Hines-Boykin R, Ash JD, et al. Tissue specificity of the Kaposi's sarcoma-associated herpesvirus latent nuclear antigen (LANA/orf73) promoter in transgenic mice. *J Virol.* 2002;76(21): 11024-11032.
12. Sin S-H, Fakhari FD, Dittmer DP. The viral latency-associated nuclear antigen augments the B-cell response to antigen in vivo. *J Virol.* 2010; 84(20):10653-10660.
13. Ballon G, Chen K, Perez R, Tam W, Cesarman E. Kaposi sarcoma herpesvirus (KSHV) vFLIP oncoprotein induces B cell transdifferentiation and tumorigenesis in mice. *J Clin Invest.* 2011; 121(3):1141-1153.
14. Chugh P, Matta H, Schamus S, et al. Constitutive NF-kappaB activation, normal Fas-induced apoptosis, and increased incidence of lymphoma in human herpes virus 8 K13 transgenic mice. *Proc Natl Acad Sci USA.* 2005;102(36): 12885-12890.
15. Verschuren EW, Hodgson JG, Gray JW, et al. The role of p53 in suppression of KSHV cyclin-induced lymphomagenesis. *Cancer Res.* 2004; 64(2):581-589.
16. O'Hara AJ, Vahrson W, Dittmer DP. Gene alteration and precursor and mature microRNA transcription changes contribute to the miRNA signature of primary effusion lymphoma. *Blood.* 2008;111(4):2347-2353.
17. Fakhari FD, Dittmer DP. Charting latency transcripts in Kaposi's sarcoma-associated herpesvirus by whole-genome real-time quantitative PCR. *J Virol.* 2002;76(12):6213-6223.
18. Hardy RR. B-1 B cells: development, selection, natural autoantibody and leukemia. *Curr Opin Immunol.* 2006;18(5):547-555.
19. Pillai S, Cariappa A. The follicular versus marginal zone B lymphocyte cell fate decision. *Nat Rev Immunol.* 2009;9(11):767-777.
20. Cariappa A, Boboila C, Moran ST, et al. The recirculating B cell pool contains two functionally distinct, long-lived, posttransitional, follicular B cell populations. *J Immunol.* 2007;179(4):2270-2281.
21. Cariappa A, Mazo IB, Chase C, et al. Perisinusoidal B cells in the bone marrow participate in T-independent responses to blood-borne microbes. *Immunity.* 2005;23(4):397-407.
22. Martin F, Oliver AM, Kearney JF. Marginal zone and B1 B cells unite in the early response against T-independent blood-borne particulate antigens. *Immunity.* 2001;14(5):617-629.
23. Song H, Cerny J. Functional heterogeneity of marginal zone B cells revealed by their ability to generate both early antibody-forming cells and germinal centers with hypermutation and memory in response to a T-dependent antigen. *J Exp Med.* 2003;198(12):1923-1935.
24. Baumgarth N, Herman OC, Jager GC, et al. B-1 and B-2 cell-derived immunoglobulin M antibodies are nonredundant components of the protective response to influenza virus infection. *J Exp Med.* 2000;192(2):271-280.
25. Ochsenbein AF, Fehr T, Lutz C, et al. Control of early viral and bacterial distribution and disease by natural antibodies. *Science.* 1999;286(5447): 2156-2159.
26. Wilker PR, Kohyama M, Sandau MM, et al. Transcription factor Mef2c is required for B cell proliferation and survival after antigen receptor stimulation. *Nat Immunol.* 2008;9(6):603-612.
27. Sugaya M, Watanabe T, Yang A, et al. Lymphatic dysfunction in transgenic mice expressing KSHV k-cyclin under the control of the VEGFR-3 promoter. *Blood.* 2005;105(6):2356-2363.
28. Verschuren EW, Klefstrom J, Evan GI, et al. The oncogenic potential of Kaposi's sarcoma-associated herpesvirus cyclin is exposed by p53 loss in vitro and in vivo. *Cancer Cell.* 2002;2(3): 229-241.
29. Ballestas ME, Kaye KM. The latency-associated nuclear antigen, a multifunctional protein central to Kaposi's sarcoma-associated herpesvirus latency. *Future Microbiol.* 2011;6(12):1399-1413.
30. Pillai S, Cariappa A, Moran ST. Marginal zone B cells. *Annu Rev Immunol.* 2005;23(1):161-196.
31. Della Bella S, Taddeo A, Colombo E, et al. Human herpesvirus-8 infection leads to expansion of the preimmune/natural effector B cell compartment. *PLoS ONE.* 2010;5(11):e15029.
32. Teicher B. *Tumor Models in Cancer Research.* Totowa, New Jersey: Humana Press; 2002
33. Roy D, Sin S-H, Damania B, et al. Tumor suppressor genes FHIT and WWOX are deleted in primary effusion lymphoma (PEL) cell lines. *Blood.* 2011;118(7):e32-e39.
34. Speck SH, Ganem D. Viral latency and its regulation: lessons from the gamma-herpesviruses. *Cell Host Microbe.* 2010;8(1): 100-115.
35. Fredrickson TN, Lennert K, Chattopadhyay SK, et al. Splenic marginal zone lymphomas of mice. *Am J Pathol.* 1999;154(3):805-812.
36. Du M-Q, Isaccson PG. Gastric MALT lymphoma: from aetiology to treatment. *Lancet Oncol.* 2002; 3(2):97-104.
37. Hermine O, Lefrère F, Bronowicki J-P, et al. Regression of splenic lymphoma with

villous lymphocytes after treatment of hepatitis C virus infection. *N Engl J Med.* 2002;347(2):89-94.

38. Hsi ED, Singleton TP, Svoboda SM, et al. Characterization of the lymphoid infiltrate in Hashimoto thyroiditis by immunohistochemistry and polymerase chain reaction for immunoglobulin heavy chain gene rearrangement. *Am J Clin Pathol.* 1998;110(3):327-333.
39. Parsonnet J, Isaacson PG. Bacterial infection and MALT lymphoma. *N Engl J Med.* 2004;350(3): 213-215.
40. Royer B, Cazals-Hatem D, Sibilia J, et al. Lymphomas in patients with Sjogren's syndrome are marginal zone B-cell neoplasms, arise in diverse extranodal and nodal sites, and are not associated with viruses. *Blood.* 1997;90(2): 766-775.
41. Suarez F, Lortholary O, Hermine O, et al. Infection-associated lymphomas derived from marginal zone B cells: a model of antigen-driven lymphoproliferation. *Blood.* 2006;107(8): 3034-3044.
42. Franco V, Florena AM, Iannitto E. Splenic marginal zone lymphoma. *Blood.* 2003;101(7): 2464-2472.
43. Moormann AM, Chelimo K, Sumba OP, et al. Exposure to holoendemic malaria results in elevated Epstein-Barr virus loads in children. *J Infect Dis.* 2005;191(8):1233-1238.
44. Hassman LM, Ellison TJ, Kedes DH. KSHV infects a subset of human tonsillar B cells, driving proliferation and plasmablast differentiation. *J Clin Invest.* 2011;121(2):752-768.
45. Babcock GJ, Decker LL, Volk M, et al. EBV persistence in memory B cells in vivo. *Immunity.* 1998;9(3):395-404.
46. Flaño E, Kim I-J, Woodland DL, et al. γ-Herpesvirus latency is preferentially maintained in splenic germinal center and memory B cells. *J Exp Med.* 2002;196(10): 1363-1372.
47. Coleman CB, Nealy MS, Tibbetts SA. Immature and transitional B cells are latency reservoirs for a gammaherpesvirus. *J Virol.* 2010;84(24): 13045-13052.
48. Biggar RJ, Engels EA, Whitby D, et al. Antibody reactivity to latent and lytic antigens to human herpesvirus-8 in longitudinally followed homosexual men. *J Infect Dis.* 2003;187(1):12-18.